ELSEVIER

Tectonophysics 292 (1998) 101–117

TECTONOPHYSICS

# Preliminary result of magnetotelluric soundings in the fold–thrust belt of Taiwan and possible detection of dehydration

Chien-chih Chen *, Chow-son Chen

*Institute of Geophysics, National Central University, Chungli 32054, Taiwan*

Received 8 April 1997; accepted 27 January 1998

**Abstract**

Until the magnetotelluric (MT) soundings were conducted in the last two years, there was no systematic view of the deep electric conductivity in the fold–thrust belt of the Taiwan orogen, being a typical example of arc–continental collision. Presented in this paper are the initial results and preliminary interpretation of the MT survey in Taiwan. The determinant response of the impedance tensor was calculated for inversion and Occam's inversion which could generate smooth models was mainly used for interpreting MT data at each site. The existence of a conductive zone with depths of 10–20 km beneath the Island of Taiwan is undoubtedly the most important feature found in this study. The depths are well correlated with the inferred depth of dehydration reactions of Suppe (1981) and the top of the aseismic lower crust observed by Wang et al. (1994). Thus, the authors believe that the cause of this conductive zone is probably the fluids released from dehydration reactions. Additionally, close to the Lishan fault the MT data show strong distortions which may be the result of induction in more complex three-dimensional structures. Further multi-dimensional analysis of the data is required in the future for delineating a more realistic image of the subsurface heterogeneous structure. 

*Keywords:* magnetotelluric method; fold–thrust belt; Taiwan; electrical structure; dehydration

## 1. Introduction

The Island of Taiwan is located in the active boundary between the Philippine Sea plate and the Eurasian plate. The relative plate velocity between the Philippine Sea plate and Eurasian plate is about 71 km per million year and approximately in the direction N50ºW (Seno et al., 1993). The overall plate configuration in the vicinity of Taiwan is well defined by seismicity. While the Philippine Sea plate is subducting northwestward from the Ryukyu Trench in the northeast of Taiwan, the Eurasian plate is subducting beneath the Philippine Sea plate along the Manila Trench in the south of Taiwan. Thus, Taiwan lies in the region in which the polarity of the subduction changes (Suppe, 1987).

The rapid arc–continental collision is responsible for the complex geological setting and the rugged topography. The geology and tectonics of Taiwan (Fig. 1) were described in detail in the two introductory volumes of Ho (1982, 1986). The two major tectonic provinces of Taiwan are separated by a narrow, linear feature known as the Taitung Longi-

* Corresponding author. Fax: 886-3-4222044;
E-mail: s123@sal.gep.ncu.edu.tw

0040-1951/98/$19.00 
*PII* S0040-1951(98)00059-6

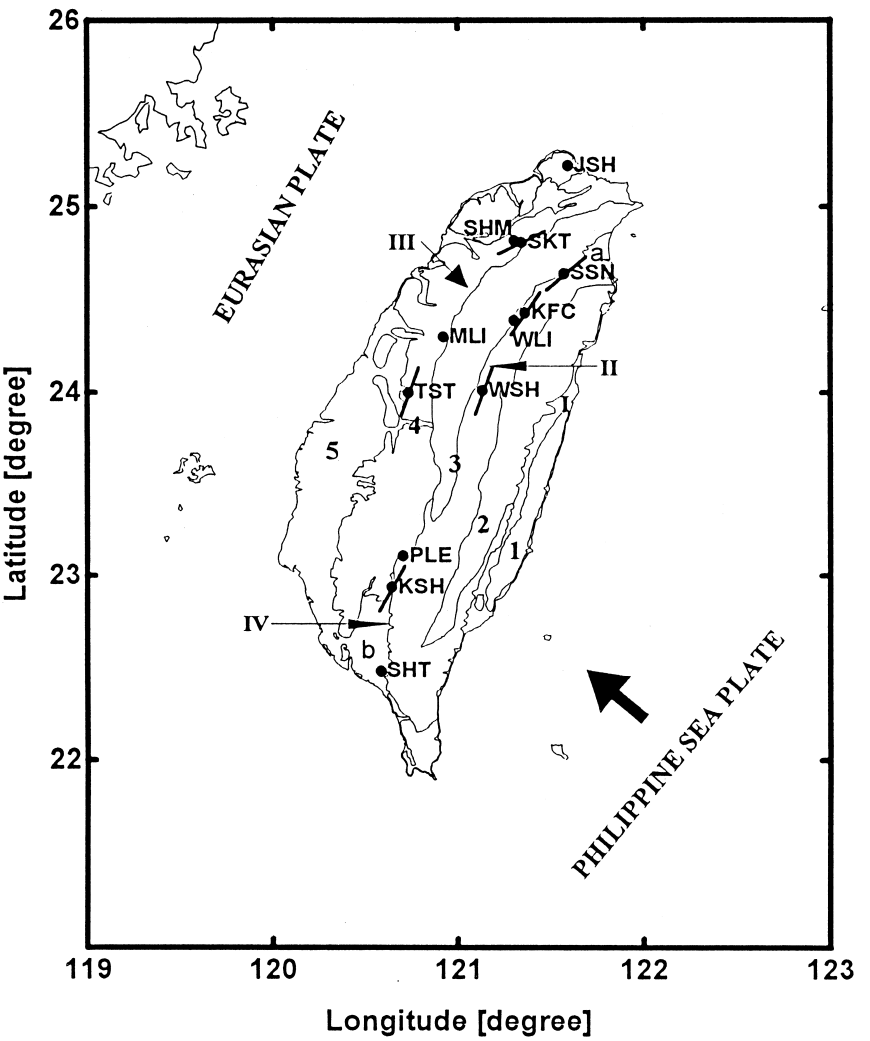


Fig. 1. The tectonic and geological structure of Taiwan. Thick arrow indicates the relative direction of plate motion. The tectonic and geological boundaries described in the text are: *I* = the Taitung Longitudinal Valley; *II* = Lishan fault; *III* = Chuchih fault; *IV* = Laonungchi fault. The geological units are: *1* = Coastal Range; *2* = eastern Central Range; *3* = western Central Range; *4* = Western Foothills; *5* = Coastal Plains; *a* = Ilan Plain; *b* = Pingtung Valley. Solid circles with names are the twelve magnetotelluric sites described in this paper. Also shown in this figure are the strikes at the period of 42.7 s from six sites which may reflect the bend in the main structure trend of Taiwan. Detailed explanation may be found in the text.

tudinal Valley. The eastern province consists of the Coastal Range and two small islands. On the other hand, the western province comprises four main subregions: (1) the metamorphic basement of the eastern Central Range; (2) the upthrust slate belt of the western Central Range; (3) the fold–thrust belt of the Western Foothills; and (4) the Coastal Plains.

The upthrust slate belt of the western Central Range is formed mainly of a thick sequence of Tertiary marine argillaceous sediments. These argillaceous sediments were altered largely to argillite, slate (the predominant rock) and phyllite after a major episode of Plio–Pleistocene orogeny or plate collision with the metamorphic grade increasing from west to east. A tectonic break in the upthrust slate belt is the boundary fault, the Lishan fault (Fig. 1). Due to the lack of detailed stratigraphic and structural analyses, many critical geological problems

are still not satisfactorily solved in the upthrust slate belt (Ho, 1982). On the contrary, the structure of the fold–thrust belt of the Western Foothills is well known through extensive deep drilling, seismic reflection profiling, and detailed surface mapping (Suppe, 1987). The Western Foothills and the Central Range are separated by the Chuchih fault in the northern part of Taiwan and the Laonungchi fault in the southern part of Taiwan. The Western Foothills are mainly composed of clastic sediments that thicken from north to south (Ho, 1986). The existence and depth of the basal decollement, if present, of the bulldozer model of Suppe (1981, 1987) may be the most important features of the tectonics of western Taiwan (Barr and Dahlen, 1989; Hwang and Wang, 1993; Wang et al., 1994; Rau and Wu, 1995).

In addition, some other important geological features with great tectonic significance should be noted, i.e. the activity of Pleistocene andesite on the northern edge of Taiwan and the two intramontane troughs including the Pingtung Valley on the southern edge of Taiwan and the Ilan Plain on the northeast edge of Taiwan. Tectonically, the Pingtung Valley is considered as a fore-arc basin or foredeep related to the Manila Trench, and the Ilan Plain is an inter-arc basin or a marginal back-arc basin of the Ryukyu arc system (Ho, 1982).

Because of its interest as a typical example of an active arc–continental collision, the structure of the active Taiwan mountain belt always catches the scientists' attention. Many geophysical investigations, including the analysis of seismicity (Wang, 1988; Wang et al., 1994), gravity measurements (Yen, 1991), seismic tomography (Rau and Wu, 1995; Ma et al., 1996) and seismic reflection profiling (Lin et al., 1997; Shih et al., 1997), have been conducted during the last decade to give a detailed figure of the geology beneath Taiwan.

Based upon the depth distribution of shallow earthquakes in Taiwan, Wang et al. (1994) reported that the depth of the brittle–quasiplastic transitional boundary of onland Taiwan may be 6 km on average. The best P-wave velocity model fitting the statistical relation between the epicentral distance and the observed apparent velocity suggests that the average crustal thickness beneath the mountain ranges is about 45 km and probably reaches up to about 50 km (Lin, 1996). The same crustal structure has also been obtained by seismic reflection profiling (Shih et al., 1997).

As another important property of the Earth's interior, unfortunately, the deep electric conductivity had not yet yielded a systematic view of Taiwan until this paper. Presented in this paper are the initial results of a series of magnetotelluric (MT) soundings which have been carried out during the last two years. Although more rigorous analyses, modellings and more extensive soundings are in progress, the preliminary results have already indicated an electric conductivity structure which is highly significant in terms of the dehydration reaction and the rheology of the crust beneath the young arc–continental orogen in Taiwan.

## 2. Results of magnetotelluric soundings

Although 37 magnetotelluric soundings have been made at locations throughout the Island of Taiwan since December 1995 and more soundings are in progress, this preliminary study concentrated on analyzing the data of the twelve sites shown in Fig. 1. Measurements were made in a nominal period range of 0.0026–110 s at each of these sites with longer-period data, to 1820 s, collected at five sites: PLE, SKT, TST, JSH and SHT. All these locations are far from the coast, more than 20 km, except the sites JSH and SHT, where for longer-period data of more than 300 s an effect of the surrounding oceans was expected.

The method of data collection and the analysis of the data are as outlined by Chen et al. (1996). The data were recorded with a real-time V5-MT-16 system (Phoenix Geophysics Ltd., Canada). The telluric field variations were measured with 50 to 100 m dipoles, in a cross-configuration, with non-polarizable Pb-PbCl electrodes. The magnetic fields were measured with coils (coil mode MTC-50, Phoenix Geophysics Ltd.) for the horizontal and vertical components. The longer-period data were generally collected over a time span of about 12 h, up to 18 h, and the shorter-period data for 4 h. The robust process (method 6 described in Jones et al., 1989) has been used to reduce the variances of the off-diagonal MT impedance for each site. As no remote referencing method (Gamble et al., 1979) has been used, the data may be subject to bias by coherent noise in either

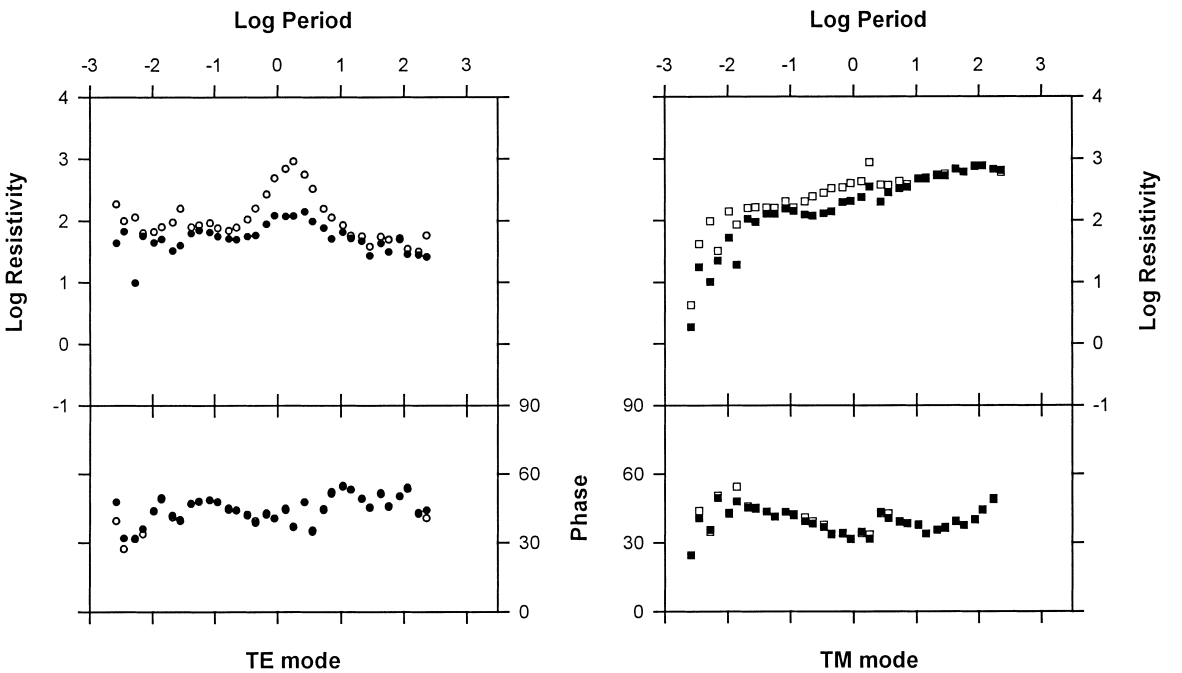


Fig. 2. The upward (open circles and squares) and downward (solid circles and squares) biased estimations of apparent resistivities and phases of the TE and TM mode from KFC. Apparent resistivities are in ohm-metres. Phases are in degrees. Periods are in seconds. For clarity uncertainties are not shown.

the magnetic or telluric fields. Fig. 2 shows upward and downward biased estimates (Sims et al., 1971; Jones et al., 1989) of apparent resistivity and phases calculated in an orientation of 20ºE from the north (approximately the principal tectonic strike of Taiwan) at one site, KFC. The characteristics of these results are broadly typical for the data at all sites. The downward biased estimates are calculated by the traditional method of calculating the elements of the impedance tensor from cross-spectral estimates. Such estimates are known to be downward biased in the presence of coherent noise in the magnetic field. The upward biased estimates were obtained by the alternative method of using cross-spectral estimates to calculate an admittance tensor which is then inverted to give the impedance. These estimates are upward biased by the presence of coherent noise in the telluric field.

As shown in Fig. 2, for the longest periods the differences between upward and downward biased estimates of the two apparent resistivities are small. For the shortest periods shown the estimates are also not dissimilar. The most obvious differences occur in the period range from 0.1 to 1 s. In this period range the upward biased E-polarization (TE mode) apparent resistivity estimates are significantly larger than the downward biased estimates. A smaller difference occurs between the upward and downward biased B-polarization (TM mode) estimates. The sharp rise in the upward biased apparent resistivity of the TE mode at around 1 s does not correspond with any sharp drop in phase and is therefore almost certainly artificial. This implies the existence of coherent noise in the measured telluric fields. In fact, in the period range of 0.1–10 s the natural signal level is lowest and the existence of any coherent noise has a much more serious effect upon the impedance estimates. The size of biased estimates for the two polarizations of the electric field depends on the exact location and orientation of the noise source (Ingham, 1996).

At a few other sites a similar distortion of apparent resistivities occurs in both the upward and downward biased estimates. A possible explanation of this is that the noise source is so close that coherent noise occurs in both the magnetic and electric fields. Where such effects are extreme, reliable

estimates of the impedance tensor can not be obtained for periods of about 1 s. The true estimate of the impedance tensor at any site necessarily lies somewhere between the upward and downward biased estimates (Ingham, 1996). However at nearly all sites in this study the downward biased estimates are clearly smoother than the upward biased ones and have been assumed as the better estimates of the true impedance tensor. This may be due to the fact that generally the magnetic field is less susceptible to measurement noise and industrial disturbances than the electric field (Pedersen, 1982).

For the purpose of an initial discussion of the magnetotelluric results, the estimates of the apparent resistivity (Fig. 3) and phase (Fig. 4) are presented in this paper in an axial system rotated to 20ºE from the geographic north, the principal tectonic strike of Taiwan. E- and B-polarizations, i.e. TE and TM modes, refer to the directions of electric fields parallel and perpendicular to this orientation, respectively. As will be discussed below, the principal directions of the impedance tensor (Fig. 5) calculated by the method of Vozoff (1972) do in fact differ from this orientation to some degrees. This orientation of the axes is chosen to provide a common axial system for the presentation and discussion of the data. The twelve sites are dealt with in groups according to their locations: (1) within the Central Range, (2) in the Western Foothills, and (3) nearby the oceans including the two sites JSH and SHT.

### *2.1. The Central Range*

Sites within the Central Range, including SSN, KFC, WLI, WSH and PLE, generally have apparent resistivities which are broadly similar to the downward biased estimates for KFC shown in Fig. 2. An exception to this is PLE, a site far from the others, and located near some geothermal area in the southern part of the Central Range.

For comparison, Fig. 6 shows curves demonstrating the variation in the apparent resistivity data at the four sites SSN, KFC, WLI and WSH. Allowing for the uncertainties, which are not shown in Fig. 6, and for a small amount of static shift in the apparent resistivities, the apparent resistivities of the TE and TM modes at all four sites are similar within a common period range. The apparent resistivities and phases (Fig. 4) from site WSH show a considerable scatter which may be a result of culture noise for periods of about 10–100 s, and from site WLI for periods longer than about 100 s.

Of much greater significance may be the departure in the TE mode apparent resistivities in the period range of 0.1–10 s among the sites SSN, KFC and WLI, which are all located close to the main boundary fault in the Central Range, the Lishan fault. For this period range there is a considerable anisotropy which may be a reflection of the lateral conductivity structure associated with the Lishan fault in the phase data at WLI (Fig. 4). However, the similar shapes of the apparent resistivity curves and the absence of obvious deviations in the phase data at SSN and KFC suggest that, should an electrical boundary be associated with the Lishan fault, then both these sites must lie on the same side of the boundary. Thus the MT results from these three sites may indicate that any electric signature of the Lishan fault is situated between KFC and WLI.

Although the strike data are scattered, it is clear that on average the trends of the principal axes of the impedance tensor at SSN, KFC and WSH are respectively above N45ºE, around N45ºE and below N45ºE (Fig. 5). The rotation of the principal axis of the impedance tensor may be due to the spectacular bend of the structural trend of the Lishan fault. It should be noted that determination of the strike angle by simple rotation of the impedance tensor is fraught with difficulty (Jones and Groom, 1993).

### *2.2. The Western Foothills*

Apparent resistivities from sites within the Western Foothills, i.e. SHM, SKT, MLI, TST and KSH, are quite different from the sites in the Central Range (Fig. 3). Although the data quality in the periods of around 10 s is poor, some important features are apparent. The main difference between these sites and those in the Central Range is that within the Western Foothills apparent resistivity values do not show an initial increase with increasing period but maintain several ten ohm-metres as the period increases. This strongly suggests the existence of a more conductive layer at depth beneath the Western Foothills. Furthermore, the apparent resistivities of the E- and B-polarizations in the longer periods from the five

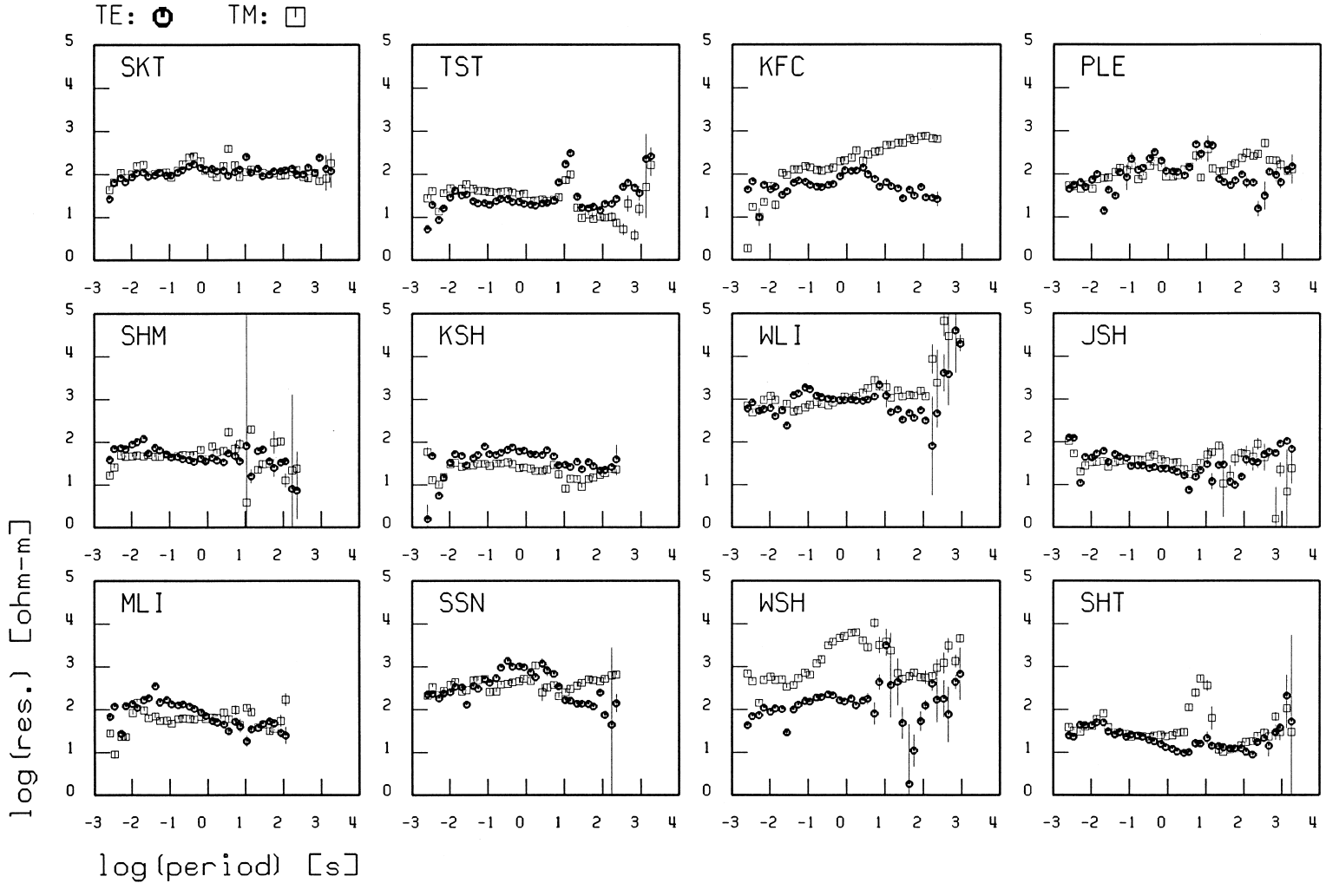


Fig. 3. The apparent resistivity of TE (circles) and TM (squares) modes from all twelve sites discussed in this paper. The first five sites, i.e. SKT, SHM, MLI, TST and KSH, are located within the Western Foothills; the following five sites, i.e. SSN, KFC, WLI, WSH and PLE, are located in the Central Range. The last two sites are nearby the surrounding oceans: JSH is located at the northern tip of Taiwan, SHT at the southern tip of Taiwan. Uncertainties, when large enough to be shown, are one standard deviation. The axial system is rotated to N20ºE.

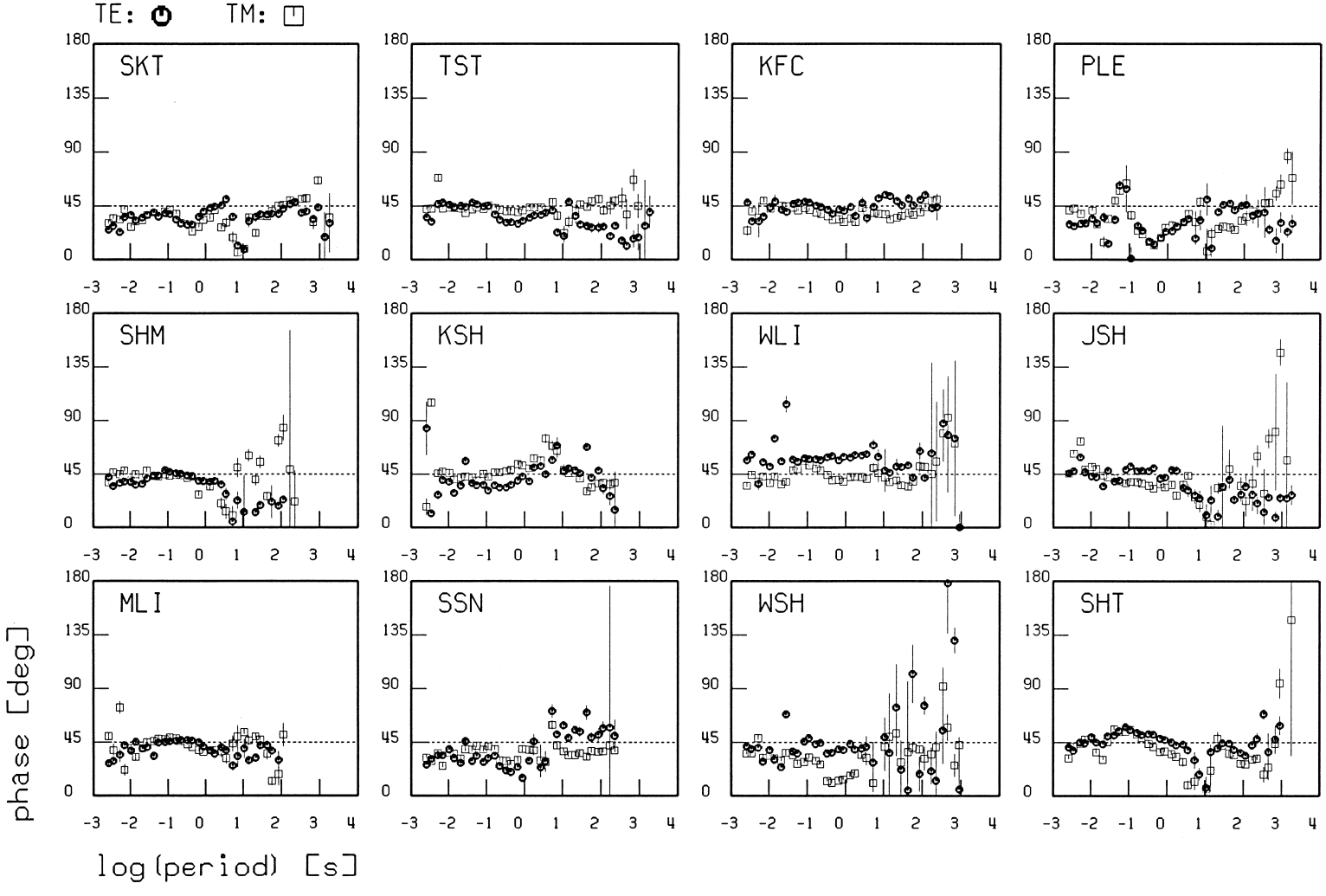


Fig. 4. The phase of the TE (circles) and TM (squares) modes from all twelve sites discussed in this paper. The first five sites, i.e. SKT, SHM, MLI, TST and KSH, are located within the Western Foothills; the following five sites, i.e. SSN, KFC, WLI, WSH and PLE, are located in the Central Range. The last two sites are nearby the surrounding oceans: JSH is located at the northern tip of Taiwan, SHT at the southern tip of Taiwan. Uncertainties, when large enough to be shown, are one standard deviation. The axial system is rotated to N20°E.

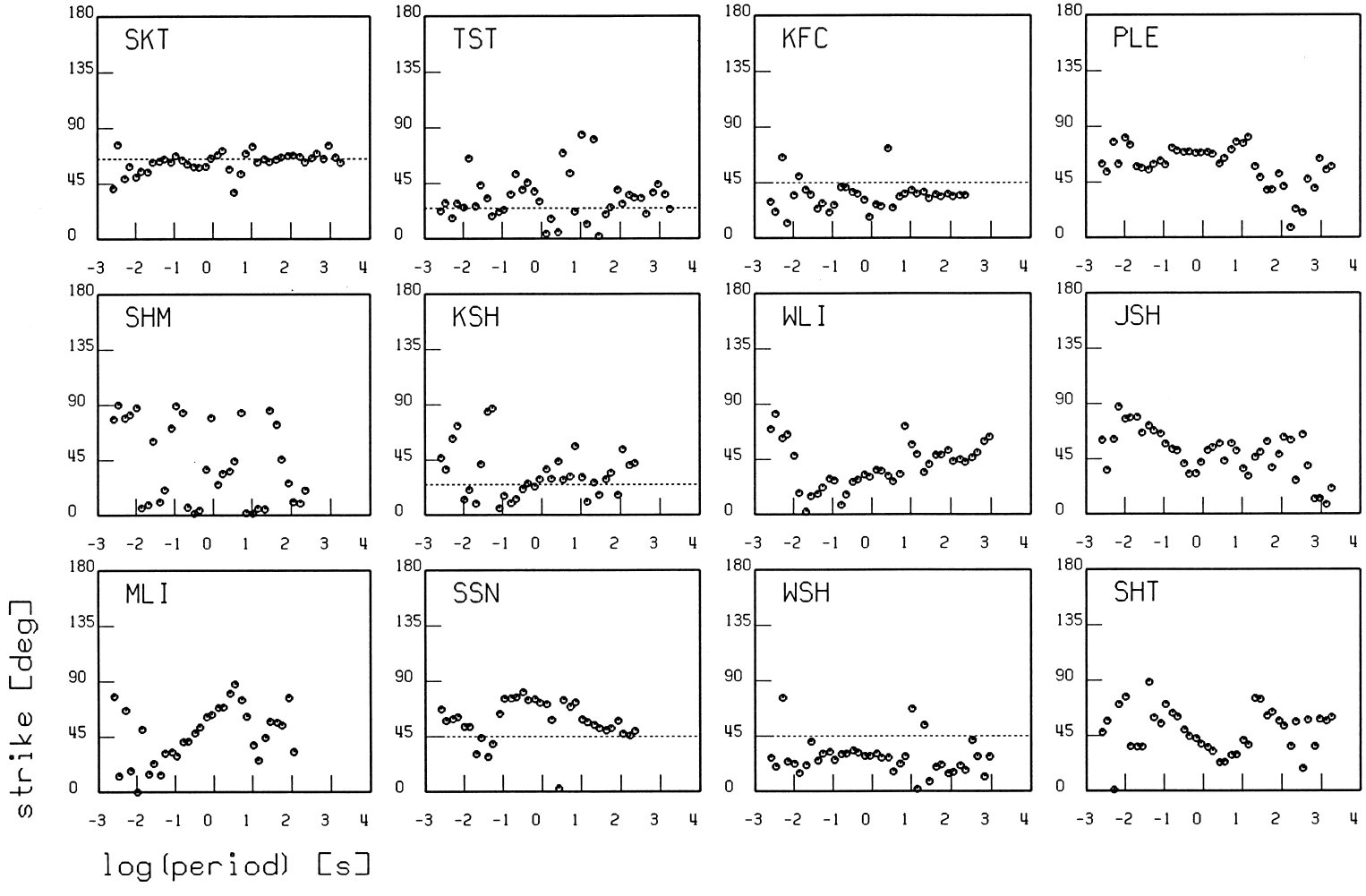


Fig. 5. The strike data, calculated by the method of Vozoff (1972), for all twelve sites discussed in this paper. The first five sites, i.e. SKT, SHM, MLI, TST and KSH, are located within the Western Foothills and arranged from north to south; the following five sites, i.e. SSN, KFC, WLI, WSH and PLE, are located in the Central Range and arranged from north to south. The last two sites are nearby the surrounding oceans: JSH is located at the northern tip of Taiwan, SHT at the southern tip of Taiwan. The dashed lines in SKT, TST and KSH have respectively strikes of 65, 25 and 25 degrees. The other dashed lines in SSN, KFC and WSH have a strike of 45 degrees. Detailed explanation can be found in the text.

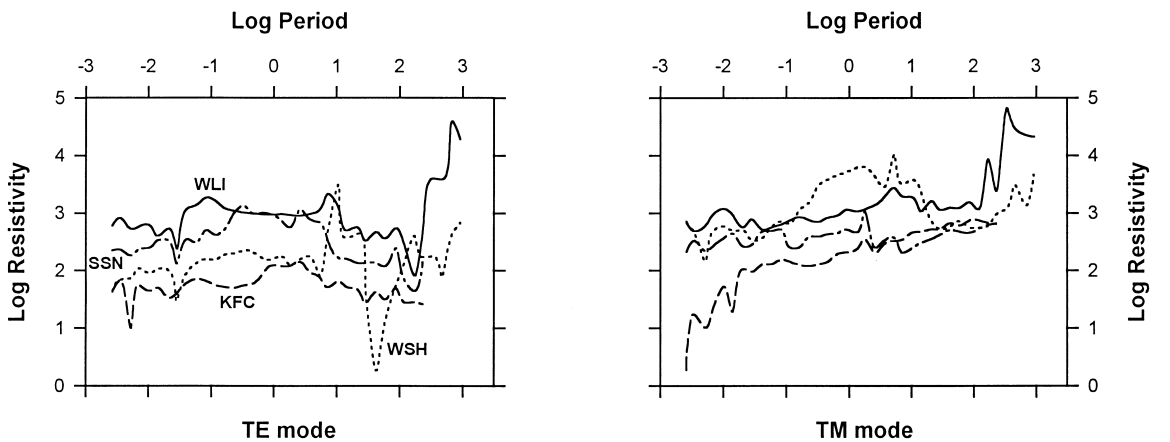


Fig. 6. Apparent resistivities of the TE and TM modes from WLI (solid line), SSN (dashed–dotted line), WSH (dotted line) and KFC (dashed line). Apparent resistivities are in ohm-metres. Periods are in seconds. For clarity uncertainties are not shown. The behaviour of the TE and TM mode apparent resistivities at four sites are similar in spite of the effect of static shift.

sites are closer to each other than those in the Central Range (Fig. 3). This may indicate that the anisotropy is stronger in the Central Range than in the Western Foothills.

Another obvious feature is the split of the apparent resistivities of the E- and B-polarizations at TST in the period range of 100–1000 s, which can also be seen in the phase data (Fig. 4) but begins at the shorter period of about 20 s. Due to the lack of data in the longer periods at site MLI, it is not possible to prove the existence of an anisotropy at greater depth in the middle part of Western Foothills of Taiwan. As the data quality is poor for the periods of around 1000 s, this feature will be not discussed further in the present paper.

While the strike data at MLI and SHM are scattered, the orientation of principal axis of the impedance tensor at SKT is about N65ºE, while those at TST and KSH are between N20ºE and N30ºE (Fig. 5). The orientation of the principal axis of the impedance tensor at SKT, TST and KSH also reflects the bend of the main structural trend in Taiwan. As Fig. 1 shows, the northern segment of Taiwan is characterized by a spectacular bend, convex to the northwest, so that from south to north all the major structural trends turn clockwise by about 55 degrees between 24ºN and 25ºN (Angelier et al., 1990). However, the southern segment of Taiwan maintains a structural trend of NNE–SSW on average.

### *2.3. Nearby the oceans: JSH and SHT*

The behaviour of the apparent resistivity and phase estimates at sites located close to the surrounding oceans (JSH and SHT) is quite complex. Fig. 7 shows the curves displaying the variation in phase data at these two sites.

One of the most obvious features is the behaviour of the B-polarization phase at JSH which rises rapidly out of the first quadrant for periods greater than 200 s. The uncertainties in the long-period B-polarization phase at JSH are large compared to those in the shorter periods; nevertheless, this striking rise in phase data is very well defined. In addition, there is a persistent difference of some 30–40º between the E- and B-polarization phases at JSH. This may be an indication of the fact that the chosen axial system (N20ºE) does not reflect the direction of the coastal line near this site which is close to N45ºW. Furthermore, the principal axis of the impedance tensor for periods greater than 1 s at JSH is very well defined at N45ºW (the strike data in Fig. 5 rotated to the fourth quadrant) coinciding well with the orientation of the coastline near JSH.

Effects of oceans on electromagnetic data have also been reported for other areas around the world. One example is South Island in New Zealand. Investigations of much longer periods in South Island were reported by Chen et al. (1993) and Chamalaun and McKnight (1993). Chen et al. (1993) presented

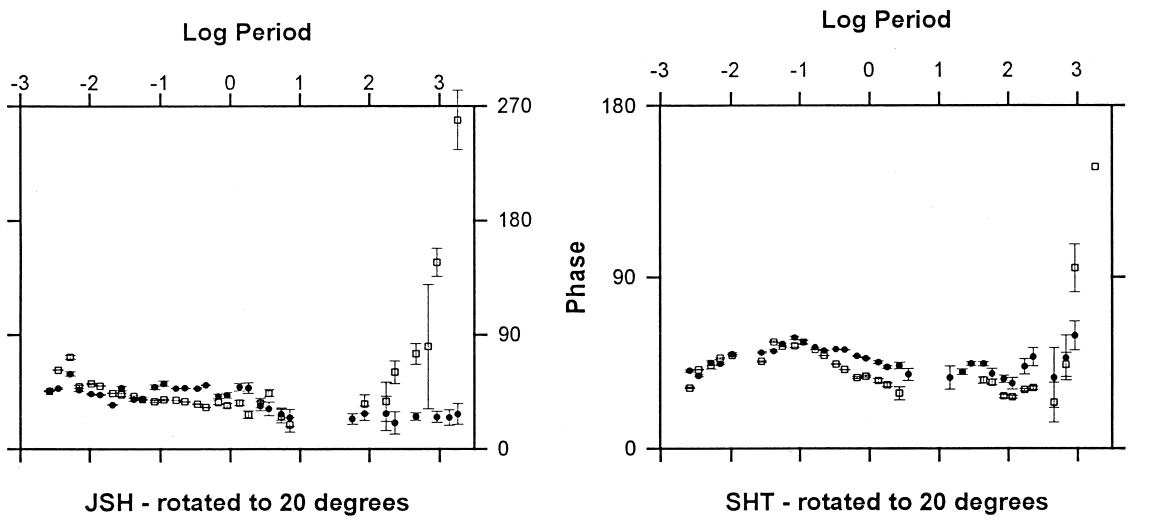


Fig. 7. E- (dots) and B-polarization (squares) phases from JSH and SHT. Phases are in degrees. Periods are in seconds. Uncertainties, when large enough to be shown, are one standard deviation. Some scattered data within the periods of about several tens of seconds have been removed for clarity. The striking rise which may be associated with the effects of the oceans at JSH is well defined.

the results of an analogue three-dimensional model study of the effects of the surrounding oceans on electromagnetic induction in South Island. For periods of magnetic variation above 5 min the effect of the oceans on the geomagnetic transfer functions is very strong. Results of a magnetometer array study covering the whole of New Zealand were reported by Chamalaun and McKnight (1993). As predicted by the analogue model for long periods of variation at which measurements were made, the measured induction arrows do respond primarily to the influence of the oceans and appear to give little indication of a subsurface conductivity structure. Also, a phase behaviour similar to that at JSH was reported for several sites in British Columbia and was interpreted in terms of an anisotropic resistivity structure (Jones, 1993; Eisel and Bahr, 1993).

There are several factors complicating this simplistic view of the results from the two sites. These factors, e.g. the topography and structure around the site, moderate the rise of the phase data for SHT and intensify the rise for JSH. The persistent difference of some 20–25° in the E- and B-polarization phases for the longer periods at SHT shown in Fig. 7 reveals a lateral variation of electrical structure near site SHT. An explanation for the behaviour of the MT sounding curves at JSH and SHT will require a considerably more detailed analysis. The results from these two sites are not discussed further in this paper.

## 3. One-dimensional inversion and modelling and electrical structure

Full interpretation of the magnetotelluric results will require a detailed analysis of possible distortions in the data (e.g. Groom and Bailey, 1989) and, at the very least, a two-dimensional modelling and inversion. However, certain inferences concerning the electrical structure, especially in the relatively near-surface, may be obtained from one-dimensional modelling and inversion. The apparent resistivities and phases used in this modelling are those calculated from the determinant impedance of Ranganayaki (1984). This parameter is invariant with rotation of the axial system. It can be shown that, only in the case where the large-scale conductivity structure is one-dimensional, does the determinant response in the presence of near-surface surficial heterogeneities have a phase unaffected by the distortions and an apparent resistivity that is purely statically shifted. For comparison, two different techniques have been used for producing one-dimensional models which give an indication of the electrical structure beneath the fold–thrust belt of Taiwan: Occam's inversion of Constable et

al. (1987), which produces models which are maximally smooth in resistivity structure, and the layered inversion with ridge regression of Inman (1975).

The results of the modelling and inversion of the determinant responses at SKT using these two techniques are shown in Fig. 8. At this site, the apparent resistivity and phase responses for both polarizations are quite similar (Figs. 3 and 4). Thus, one-dimensional modelling may give a good indication of the structure at SKT to considerable depths. Rotation of the impedance tensor shows that this similarity for both polarizations is very dependent on the orientation of the axial system and only occurs over a very narrow range centred at N20ºE. While the Occam

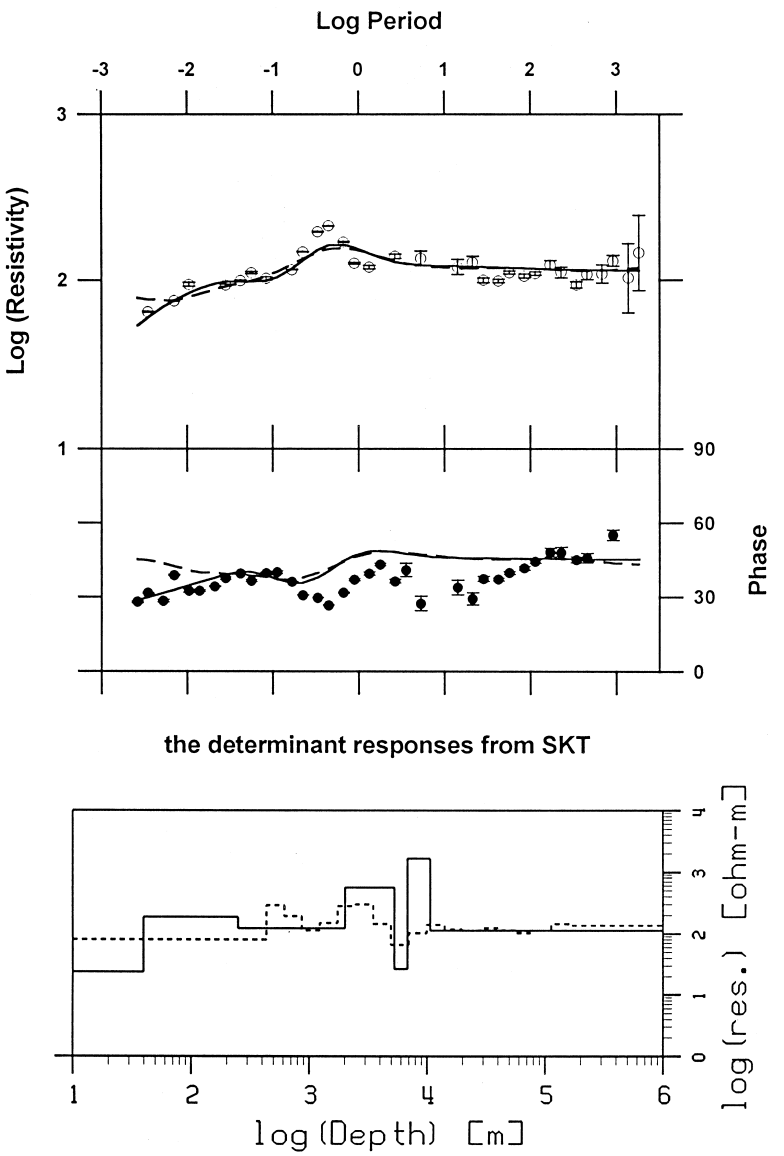


Fig. 8. One-dimensional modelling of the determinant responses from SKT. Resistivities are in ohm-metres. Phases are in degrees. Periods are in seconds. Depths are in metres. Uncertainties are one standard deviation. The solid line is the layered model using the technique of Inman (1975), the dashed line the Occam smooth inversion. Both models indicate the existence of a good conductor with a resistivity of around 40 Ω m at a depth of about 7 km.

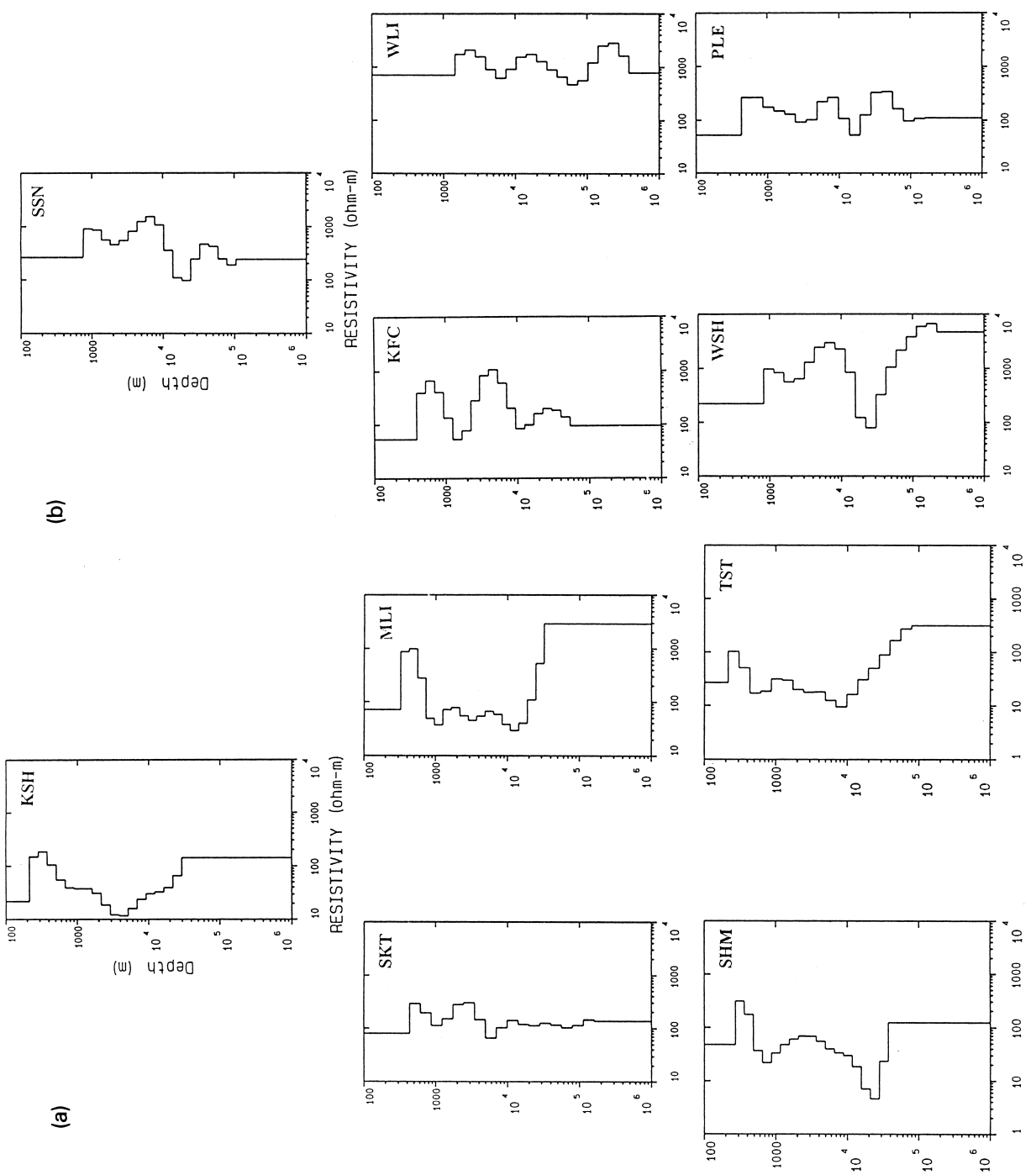
(a)
KSH
SKT
MLI
TST
SHM
(b)
SSN
KFC
WLI
WSH
PLE
Depth (m)
RESISTIVITY (ohm-m)

inversion fits the data set with a fitting error of 0.13, the simpler 7-layer resistivity model obtained with the method of Inman (1975) fits the data with a fitting error of 0.12. Both models indicate very clearly the existence of a good conductor with a resistivity of around 40 Ω m at about 7 km depth. Although there is a significant discrepancy between calculated and observed phase curves at periods between 0.1 and 100 s, the trends of these curves are similar. A upward concavity occurs between 0.1 and 1.0 s and a downward concavity between 1.0 and 10 s. The sensitivity of phase data to culture noise, particularly in the dead band, or the inconsistency between the real earth and the layered earth model, may result in a misfit at periods between 0.1 and 100 s.

### *3.1. The smooth models*

This indication of a good conductor at depth is given firm support by the smooth modelling of the determinant responses at the other sites. The Occam inversions for all ten sites are shown in Fig. 9. Although the data are slightly more scattered at some sites than at others and the fit to the determinant responses is not always quite as good as at SKT (e.g. TST has the worst fitting error of 0.3), the indications of a conductive structure at similar depths are unambiguous. As shown in Fig. 9, a conductive region exists generally beneath both the Western Foothills and the Central Range. The depth and resistivity of this conductive zone beneath the Western Foothills with average values of 9 km and 30 Ω m, respectively, show a little difference when they are compared with those beneath the Central Range, being 20 km and 80 Ω m.

There is also a suggestion from MT soundings of a second common conducting layer at around 1–3 km depth. Such a layer beneath the Western Foothills is not, however, as pronounced as that beneath the Central Range.

Local differences in near-surface resistivity do exist between the Western Foothills with a resistivity of about several tens of ohm-metres (Fig. 9a), and the Central Range with several hundreds ohm-metres (Fig. 9b). On the other hand, the deep resistivities beneath the whole of Taiwan are quite similar except for some sites, e.g. WSH, which may be affected by the effect of static shift. Estimates of depth and resistivity are dependent upon the amount of static shift to which the apparent resistivity curves have been subjected. Precluding the seriously affected sites, the depth of this moderately conductive (or resistive, for the Western Foothills) layer with a resistivity range of 100–200 Ω m are, respectively, about 55 km and 35 km for the Central Range and the Western Foothills. Thus, from the results of one-dimensional modelling of these MT soundings it can be concluded that two electric structures exist in Taiwan, which can be correlated to the two main tectonic provinces.

Results of the one-dimensional Occam inversion for the Western Foothills and Central Range described above reveal lateral variations between the two main provinces in Taiwan. In addition, one thing is worth noticing in these results. The derived models for sites within the Western Foothills, e.g. TST, show that, if dividing the whole into two parts at a depth of 35 km, the layer at the shallower depth is more conductive than the deeper one. The significance of this conductive crust will be discussed in the next section.

### *3.2. The layered models*

The Occam inversion has provided, in a special sense, the only and smoothest model whose features are the essential characteristics of any possible solution (Constable et al., 1987), but the field MT data have also been inverted with the ridge regression technique (Inman, 1975) to provide the bounds of resistivity and depth of this layer and to study the unambiguity of the highly conductive layer (HCL) in the crust.

Figs. 10 and 11 are simple layered inversions from the ridge regression technique at six sites located in the Western Foothills and the Central Range. The bounds of resistivity and depth of each layer, obtained from the equivalent analysis of a parameter

Fig. 9. Occam smooth inversions of determinant responses from sites located on (a) the Western Foothills and (b) the Central Range. Detailed explanation of the results can be found in the text.

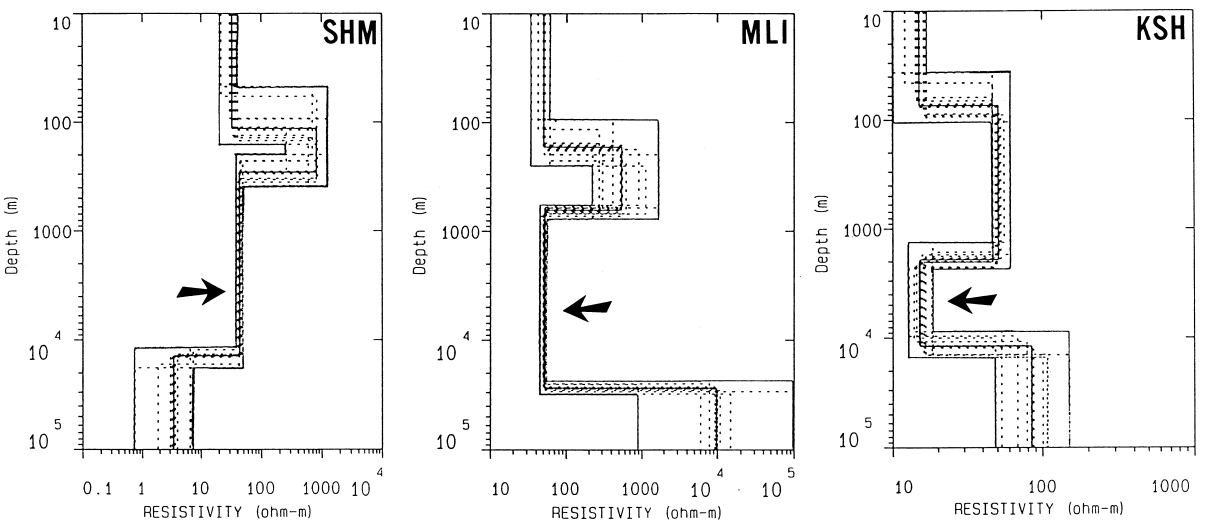


Fig. 10. Layered inversions with ridge regression of determinant responses from three selected sites located in the Western Foothills. The middle solid line shows the best model and the two outer solid lines show the limits of resistivity and depth for each layer. The dashed lines are several equivalent models. Detailed explanations of equivalent analyses may be found in the text. Arrow indicates the highly conductive layer with a conductance of several hundreds of siemens at each site.

resolution matrix, are also shown in these figures. The parameter resolution matrix is a byproduct of the ridge regression inverse modelling algorithm and gives an indication as to how well each of the inverted parameters is resolved (Inman, 1975). The equivalent analysis tests the parameter changes indicated by the resolution matrix. If the resolution matrix shows the linear combinations of the known parameters, then the resolution matrix minus the identity matrix shows the linear combinations of the unknown parameters. Varying the parameters along these paths does not increase the fitting error, as long

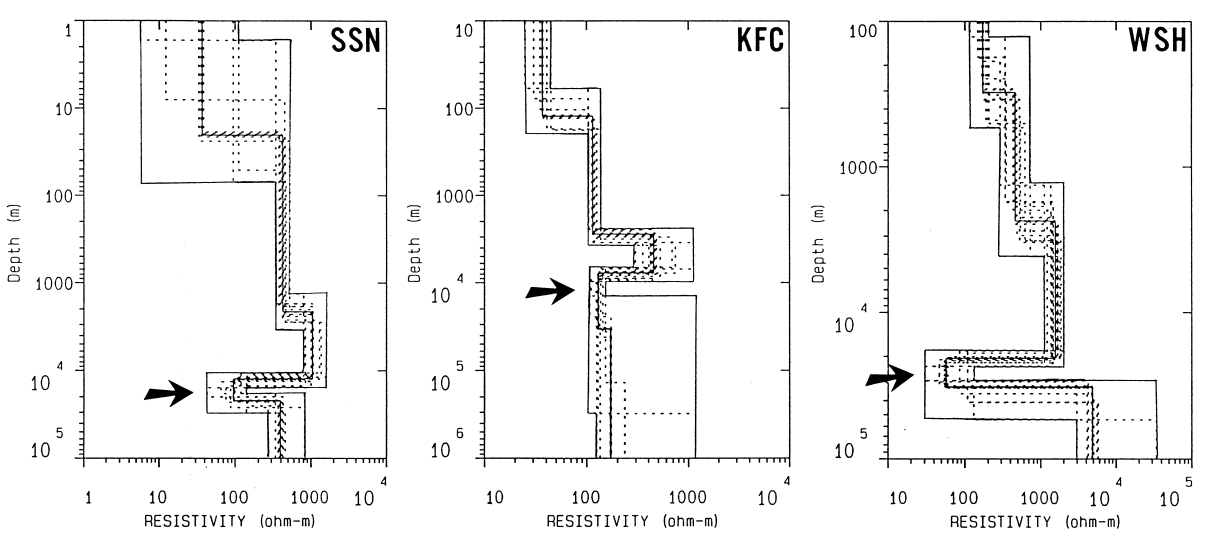


Fig. 11. Layered inversions with ridge regression of determinant responses from sites located in the Central Range. The middle solid line shows the best model and the two outer solid lines show the limits of resistivity and depth for each layer. The dashed lines are several equivalent models. Detailed explanations of equivalent analyses may be found in the text. Arrow indicates the highly conductive layer with a conductance of several hundreds of siemens at each site.

as the changes are not large. The equivalent analysis tests the range of this variation in parameters and finds the various equivalent models that could also give valid solutions for the inverse problem.

According to the result of the Occam inversion, the three sites within the Western Foothills, i.e. SHM, MLI and KSH, have been inverted using a simpler 4-layer resistivity model (Fig. 10), while the sites within the Central Range, i.e. SSN, KFC and WSH, have been inverted using a simpler 5-layer model (Fig. 11). The resistivity and thickness of the HCL in all six sites are on average several tens of ohm-metres and about 10 km, respectively, corresponding with a conductance of of several hundreds of siemens. The resolution of both resistivity and thickness for HCL is quite high.

While the bounds of resistivity and depth of HCL had been obtained from the layered inversion and the enhanced conductivity in the crust had been confirmed by this inverted algorithm, the inverted ridge regression technique gives no clear bounds of neither the resistivity nor the depth for the deeper electrical basement. This may be because that the selected six sites are almost with shorter-period data or that the reliability of longer-period data is doubtful (Figs. 3 and 4). Thus, a better knowledge of the deeper structure must await more reliable data or a fuller interpretation.

## 4. Discussion and conclusions

The indication of a conductive region at a depth of about 9 and 20 km for the Western Foothills and Central Range, respectively, is clearly the most important feature of these preliminary results which have been obtained. The conductive region may have its origin in mobilization of fluids and enhanced temperature beneath Taiwan.

It is possible that enhanced temperature leads to a higher electrical conductivity than normal in the upper crust beneath Taiwan. However, an increase of temperature at a depth of 9 km beneath the Western Foothills with only about 300ºC or less, based on petroleum exploration (Suppe, 1981), cannot be sufficient to produce a significant conductivity anomaly (fig. 6 of Chen et al., 1996, or Chapter 3 of Zhdanov and Keller, 1994). A detectable anomaly in the upper crust beneath the Western Foothills in Taiwan would probably require the presence of fluids. One origin of fluids is possibly the dehydration of greenschists (e.g. Brown, 1994). This has previously been invoked as an explanation for the common occurrence of good conductors in the continental crust (Jones, 1987; Hyndman et al., 1993). It has been expected by Suppe (1981) that dehydration reactions are taking place at a lower temperature of about 220ºC at a depth of 7 km in the Western Foothills due to a drop in the fluid pressure–solid pressure ratio.

The excess pore-fluid pressure may be an indirect indication of the presence of water beneath the Western Foothills (Suppe, 1981). The existence of inter-granular films of water containing as little as 1% of fluid can substantially lower the electrical conductivity as a function of porosity (Hyndman and Shearer, 1989; Hyndman et al., 1993), and may be expected to occur at or below the brittle–ductile transition (Bailey, 1990; Holness, 1993). Consequently, there are grounds for anticipating that the existence of a delamination surface (Koons, 1990) might be associated with a layer of anomalously high electrical conductivity. As expected, the top of the conductive region, at about 10–20 km depth, obtained by MT soundings, corresponds with the top of the aseismic zone found by Wang et al. (1994).

Greenschist–zeolite facies rocks in the Central Range occur at approximately 15 km depth and may be raised and crop out by imbricated upthrusting caused by the collision of the Philippine Sea plate with the Eurasian continental plate (Chen and Wang, 1995). The continuing uplift, with the topographic height of the Central Range remaining approximately constant by the rapid erosion rate, maintains the enhanced temperature in the main region of uplift (Teng, 1990) and allows a lateral migration of isotherms. This not only prevents rehydration through cooling but may also release water into the upper crust with increasing distance from the principal region of uplift.

More knowledge of the Central Range could help to define the thermal and rheological structure of this province so that the many critical geological problems could be solved in the upthrust slate belt. If the conductive zone at a depth of about 20 km beneath the Central Range could be correlated to the other one beneath the Western Foothills, and the effect of static shift in the one-dimensional modelling is not

too serious, dehydration reactions would take place at 13–24 km depth as obtained by magnetotelluric soundings. This implication seems consistent with the study of the depth distribution of shallow earthquakes (Wang et al., 1994) which revealed that the seismicity is quite low below a depth of 12 km in the Central Range.

There is no better indication that the electrical basement appearing at all sites with a uniform resistivity of about 100–200 Ω m reflects the Moho, than the fact that the depth of the electrical basement agrees with the crustal thickness in the Central Range obtained by the study of arrival differences of first P-waves proposed by Lin (1996). While the conductive basement in the Central Range is at a depth of about 55 km, the P-wave velocity model suggests that the average depth of the Moho beneath the mountain ranges in Taiwan probably reaches about 50 km (Lin, 1996). The layered models could not clearly indicate the bounds of resistivity and depth of this electrical basement, while the smooth models do. Conclusions on the deeper structure must await more reliable data or a fuller interpretation.

It should be noted that the results from sites within the Central Range contain more or less the effects of a static shift due to the near-surface abnormal structure. Although the determinant impedance of Ranganayaki (1984) is capable of separating the near-surface resistivity variation from the variations at depth and finding the relative resistivity variations with depth, the results should still possibly be shifted for both depth and resistivity. Results from KFC and WLI provide a good illustration. As described above, the apparent resistivity curve at WLI was subjected to the effect of the Lishan fault (Fig. 3). However, the inverted model of the determinant response from WLI is really similar to that from KFC, as shown in Fig. 7b, and the depths and resistivities of the model from WLI are obviously shifted.

In a further analysis of the data the distortions due to near-surface inhomogeneities should be taken into account (e.g. Groom and Bailey, 1989; Groom and Bahr, 1992). A subsequent two-dimensional modelling and inversion should then provide a much clearer indication of any such conductive structure beneath the Western Foothills. This should also yield a much better resolution of the structure beneath the Central Range and adjacent to the Lishan fault and more detailed information on the relationship between the electrical, thermal and rheological structures of the Taiwan orogen.

## Acknowledgements

This work was mainly supported by the National Science Council of R.O.C. under the grants NSC84-2111-M-008-041 and NSC86-2116-M-008-005, and partially supported by National Central University. The authors wish to thank especially Mr. G. Graham of Phoenix Geophysics Ltd. (Canada) for the field training in MT surveying during December, 1995, and many individuals who participated in the field works. The authors wish to thank Drs H. Utada and K. Bahr for critical comments on an earlier version of the manuscript.

## References

Angelier, J., Bergerat, F., Chu, H.T., Lee, T.Q., 1990. Tectonic analysis and the evolution of a curved collision belt: the Hsuehshan Range, northern Taiwan. Tectonophysics 183, 77–96.

Bailey, R.C., 1990. Trapping of aqueous fluids in the deep crust. Geophys. Res. Lett. 17, 1129–1132.

Barr, T.D., Dahlen, F.A., 1989. Steady-state mountain building, 2. Thermal structure and heat budget. J. Geophys. Res. 94, 3923–3947.

Brown, C., 1994. Tectonic interpretation of regional conductivity anomalies. Surv. Geophys. 15, 123–158.

Chamalaun, F.H., McKnight, J.D., 1993. A New Zealand wide magnetometer array study. J. Geomagn. Geoelectr. 45, 741–759.

Chen, C.C., Chen, C.S., Chou, K., 1996. A study of thermal structure using magnetotellurics. Proc. Geol. Conf. in Memory of Prof. T.P. Yen, Chungli, pp. 123–131 (in Chinese).

Chen, C.H., Wang, C.H., 1995. Explanatory Notes for the Metamorphic Facies Map of Taiwan. Central Geological Survey, MOEA, Taipei, 2nd ed., 51 pp. (in Chinese).

Chen, J., Dosso, H.W., Ingham, M., 1993. Electromagnetic induction in the New Zealand South Island. Phys. Earth Planet. Inter. 81, 253–260.

Constable, S.C., Parker, R.L., Constable, C.G., 1987. Occam's inversion: a practical algorithm for generating smooth models from electromagnetic sounding data. Geophysics 52, 289–300.

Eisel, M., Bahr, K., 1993. Electrical anisotropy in the lower crust of British Columbia: an interpretation of a magnetotelluric profile after tensor decomposition. J. Geomagn. Geoelectr. 45, 1115–1126.

Gamble, T., Goubau, W., Clarke, J., 1979. Magnetotellurics with a remote magnetic reference. Geophysics 44, 53–68.

Groom, R.W., Bahr, K., 1992. Corrections for near surface effects: decomposition of the magnetotelluric impedance tensor

and scaling corrections for regional resistivities: a tutorial. Geophys. Surv. 13, 341–380.

Groom, R.W., Bailey, R.C., 1989. Decomposition of magnetotelluric impedance tensor in the presence of local three-dimensional galvanic distortion. J. Geophys. Res. 94, 1913–1925.

Ho, C.S., 1982. Tectonic Evolution of Taiwan, Explanatory Text of the Tectonic Map of Taiwan. Ministry of Economic Affairs, Taipei, 126 pp.

Ho, C.S., 1986. An Introduction to the Geology of Taiwan, Explanatory Text of the Geological Map of Taiwan. Ministry of Economic Affairs, Taipei, 2nd ed., 164 pp. (in Chinese).

Holness, M.B., 1993. Temperature and pressure dependence of quartz–aqueous fluid dihedral angles: the control of adsorbed $H_2O$ on the permeability of quartzites. Earth Planet. Sci. Lett. 117, 363–377.

Hwang, W.T., Wang, C.Y., 1993. Sequential thrusting model for mountain building: constraints from geology and heat flow of Taiwan. J. Geophys. Res. 98, 9963–9973.

Hyndman, R.D., Shearer, P.M., 1989. Water in the lower continental crust: modeling magnetotelluric and seismic reflection results. Geophys. J. Int. 98, 343–365.

Hyndman, R.D., Vanyan, L.L., Marquis, G., Law, L.K., 1993. The origin of electrically conductive lower crustal continental crust: saline water or graphite? Phys. Earth Planet. Inter. 81, 325–344.

Ingham, M., 1996. Magnetotelluric soundings across the Southern Alps orogen, South Island of New Zealand: data presentation and preliminary interpretation. Phys. Earth Planet. Inter. 94, 253–260.

Inman, J.R., 1975. Resistivity inversion with ridge regression. Geophysics 40, 798–817.

Jones, A.G., 1987. MT and reflection: an essential combination. Geophys. J.R. Astron. Soc. 89, 7–18.

Jones, A.G., 1993. The BC87 dataset: tectonic setting, previous em results and recorded MT data. J. Geomagn. Geoelectr. 45, 1089–1105.

Jones, A.G., Groom, R.W., 1993. Strike angle determination from the magnetotelluric impedance tensor in the presence of noise and local distortion: rotate at your peril! Geophys. J. Int. 113, 524–534.

Jones, A.G., Chave, A.D., Egbert, G., Auld, D., Bahr, K., 1989. A comparison of techniques for magnetotelluric response function estimation. J. Geophys. Res. 94, 14201–14213.

Koons, P.O., 1990. Two-sided orogen: collision and erosion from the sandbox to the Southern Alps, New Zealand. Geology 18, 679–682.

Lin, C.H., 1996. Crustal structures estimated from arrival differences of the first P-waves in Taiwan. J. Geol. Soc. China 39, 1–12.

Lin, C.H., Yeh, Y.H., Shih, R.C., Yen H.Y., Huang, B.S., 1997. Investigation of deep crustal structures from wide-angle seismic data in the Taiwan area. In: Program and Expanded Abstracts of the 1997 Annual Meeting of Geological Society of China, Nat. Cheng-kung Univ., Tainan, pp. 376–378.

Ma, K.F., Wang, J.H., Zhao, D., 1996. Three-dimensional seismic velocity structure of the crust and uppermost mantle beneath Taiwan. J. Phys. Earth 44, 85–105.

Pedersen, L.B., 1982. The magnetotelluric impedance tensor — its random and bias errors. Geophys. Prospect. 30, 188–210.

Ranganayaki, R.P., 1984. The interpretive analysis of magnetotelluric data. Geophysics 49, 1730–1748.

Rau, R.J., Wu, F.T., 1995. Tomographic imaging of lithospheric structures under Taiwan. Earth Planet. Sci. Lett. 133, 517–532.

Seno, T., Stein, S., Gripp, A.E., 1993. A model for the motion of the Philippine Sea plate consistent with NUVEL-1 and geological data. J. Geophys. Res. 98, 17941–17948.

Shih, R.C., Yeh, Y.H., Lin, C.H., Yen H.Y., Huang, B.S., Liu, C.S., 1997. Results of onshore–offshore deep seismic profiling in Taiwan. In: Program and Expanded Abstracts of the 1997 Annual Meeting of Geological Society of China, Nat. Cheng-kung Univ., Tainan, pp. 385–389 (in Chinese).

Sims, W.E., Bostick, F.X., Smith, H.W., 1971. The estimation of magnetotelluric impedance tensor elements. Geophysics 36, 938–942.

Suppe, J., 1981. Mechanics of mountain building and metamorphism in Taiwan. Mem. Geol. Soc. China 4, 67–89.

Suppe, J., 1987. The active Taiwan mountain belt. In: The Anatomy of Mountain Ranges. Princeton Univ. Press, Princeton, N.J., pp. 277–293.

Teng, L.S., 1990. Geotectonic evolution of late Cenozoic arc–continental collision in Taiwan. Tectonophysics 183, 57–76.

Vozoff, K., 1972. The magnetotelluric method in the exploration of sedimentary basins. Geophysics 37, 98–141.

Wang, J.H., 1988. b-values of shallow earthquakes in Taiwan. Bull. Seismol. Soc. Am. 78, 1243–1254.

Wang, J.H., Chen, K.C., Lee, T.Q., 1994. Depth distribution of shallow earthquakes in Taiwan. J. Geol. Soc. China 37, 125–142.

Yen, H.Y., 1991. Gravity Anomalies in Taiwan and their Tectonic Implications. Ph.D. thesis. Nat. Central Univ., Chungli, 98 pp. (in Chinese).

Zhdanov, M.S., Keller, G.V., 1994. The Geoelectrical Methods in Geophysical Exploration. Elsevier, Amsterdam, 873 pp.